interaction. Finally, in this study, we illustrate how miRNA regulation by probiotics may lead to enhanced IL-10 production and partly explain the anti-inflammatory effects observed in clinical trials with specific probiotic strains.

Audrey Demont, BS
Feriel Hacini-Rachinel, PhD
Rémi Doucet-Ladevèze, MS
Catherine Ngom-Bru, PhD
Annick Mercenier, PhD
Guénolée Prioult, PhD
Carine Blanchard, PhD

From Nutrition and Health Research, Nestlé Research Center, Lausanne, Switzerland.
E-mail: Carine.Blanchard@rdls.nestle.com.

REFERENCES

1. de Moreno de LA, del CS, Zurita-Turk M, Santos RC, van de Guchte M, Azevedo V, et al. Importance of IL-10 modulation by probiotic microorganisms in gastrointestinal inflammatory diseases. ISRN Gastroenterol 2011;2011:892971.
2. Smelt MJ, de Haan BJ, Bron PA, van SI, Meijerink M, Wells JM, et al. *L. plantarum, L. salivarius,* and *L. lactis* attenuate Th2 responses and increase Treg frequencies in healthy mice in a strain dependent manner. PLoS One 2012; 7:e47244.
3. Taverniti V, Guglielmetti S. The immunomodulatory properties of probiotic microorganisms beyond their viability (ghost probiotics: proposal of paraprobiotic concept). Genes Nutr 2011;6:261-74.
4. Powell MJ, Thompson SA, Tone Y, Waldmann H, Tone M. Posttranscriptional regulation of IL-10 gene expression through sequences in the 3′-untranslated region. J Immunol 2000;165:292-6.
5. Xie N, Cui H, Banerjee S, Tan Z, Salomao R, Fu M, et al. MicroRNA-27a regulates imflamatory response of macrophages by targeting interleukin 10. J Immunol 2014;193:327-34.
6. Yeh CH, Chen TP, Wang YC, Lin YM, Fang SW. MicroRNA-27a regulates cardiomyocytic apoptosis during cardioplegia-induced cardiac arrest by targeting interleukin 10-related pathways. Shock 2012;38:607-14.
7. Zhang L, Hou D, Chen X, Li D, Zhu L, Zhang Y, et al. Exogenous plant MIR168a specifically targets mammalian LDLRAP1: evidence of cross-kingdom regulation by microRNA. Cell Res 2012;22:107-26.

A histamine-independent itch pathway is required for allergic ocular itch

To the Editor:

Itch is the cardinal symptom of allergic conjunctivitis and afflicts 15% to 20% of the population worldwide. Histamine produced by conjunctival mast cells has been implicated as the principal itch mediator that activates histamine receptors on primary sensory fibers to induce allergic ocular itch.[1] However, antihistamines cannot completely relieve ocular itch in many cases, suggesting the involvement of a histamine-independent itch pathway. Herein, we sought to identify the histamine-independent neural pathway involved in allergic conjunctivitis and to develop new therapeutic strategies for allergic ocular itch.

Allergic ocular itch typically originates from the conjunctiva, a mucosal membrane that is anatomically distinct from the skin and covers the ocular surface over the sclera and the inner surface of the eyelid. However, our knowledge about the neural regulations of allergic ocular itch and its difference from skin itch is limited.

Mast cells have been shown to secrete many bioactive compounds in addition to histamine.[2,3] Yet, the contribution of histamine-independent mediators to allergic ocular itch in comparison to histamine, and the neural pathway mediating the histamine-independent components in ocular itch remain unclear. TRPA1 is a cation channel that is often colocalized with TRPV1 in a subpopulation of primary sensory neurons in the trigeminal ganglion (TG) and the dorsal root ganglion. TRPV1 is known to be the downstream transduction channel of histamine H1 receptor in sensory neurons.[4] TRPA1 was recently found to be the downstream transduction channel of histamine-independent itch in the skin.[5] However, it is yet unknown whether TRPA1 is required for mast cell–mediated allergic itch. In this study, we characterized the role of TRPA1 as a histamine-independent modulator in ocular itch associated with allergic conjunctivitis.

To delineate the respective role of TRPA1 and TRPV1 in ocular itch, we first examined the acute behavioral responses of wild-type (WT), TRPA1 knockout (KO), and TRPV1 KO mice to pruritogens applied directly to their lower conjunctival sacs. We were able to differentiate ocular itch from pain using our behavioral models, in which itch-inducing compounds provoked mice to scratch the treated area using their hindpaw, whereas pain-inducing capsaicin elicited wiping behavior using the forelimb (Fig 1, *A*). We found that histamine challenge (46 μg in 2.5 μL PBS) induced 15 ± 1.8 scratching bouts in WT and 14.7 ± 3 scratching bouts in TRPA1 KO mice (Fig 1, *B*), but significantly less itch responses in TRPV1 KO mice (5 ± 1.3 bouts), suggesting that TRPV1—rather than TRPA1—is responsible for histamine-dependent ocular itch signaling. We then tested 2 histamine-independent pruritogens, chloroquine and serotonin, on evoking ocular itch. Chloroquine-induced (12.4 μg) ocular scratching was significantly decreased in TRPA1 KO mice (6.3 ± 1.1 bouts), compared with WT (16.6 ± 2 bouts) and TRPV1 KO mice (14.3 ± 2.3 bouts) (Fig 1, *C*), indicating that TRPA1 is required for histamine-independent itch induced by chloroquine. In contrast, there was no difference in ocular itch responses induced by serotonin (0.2 μg) among WT (11.1 ± 1.1 bouts), TRPA1 KO (12.3 ± 1.0 bouts) and TRPV1 KO mice (11.6 ± 1 bouts) (Fig 1, *D*). Vehicle control (PBS) induced only minimal scratching responses (Fig 1, *E*). These behavioral results indicate a pivotal role of TRPA1 in certain types of nonhistaminergic ocular itch.

To further explore the underlying mechanisms, we examined whether TRPA1 is functionally required for the responsiveness of conjunctival sensory fibers to pruritogens. We found that the conjunctival mucosa is abundantly innervated by TRPA1$^+$ and TRPV1$^+$ neurons, but not cold-sensing TRPM8$^+$ neurons, in TG (see Fig E1 in this article's Online Repository at www. jacionline.org). GCaMP3-assisted calcium imaging of conjunctival sensory fibers showed that on stimulation by pruritogens, subpopulations of conjunctival nerve fibers displayed moderate to high calcium mobilization (Fig 1, *F-K*). Interestingly, TRPA1 deficiency does not affect conjunctival nerve response to histamine stimulation, but significantly reduces the nerve response to chloroquine stimulation. In contrast, TRPV1 is required for nerve fiber response to histamine but not to chloroquine in the conjunctiva. Finally, deficiency in TRPA1 or TRPV1 did not affect serotonin-induced nerve activity (Fig 1, *L*). These data reveal a segregation of TRPA1-dependent and TRPV1-dependent pathways in conjunctiva-innervating sensory neurons.
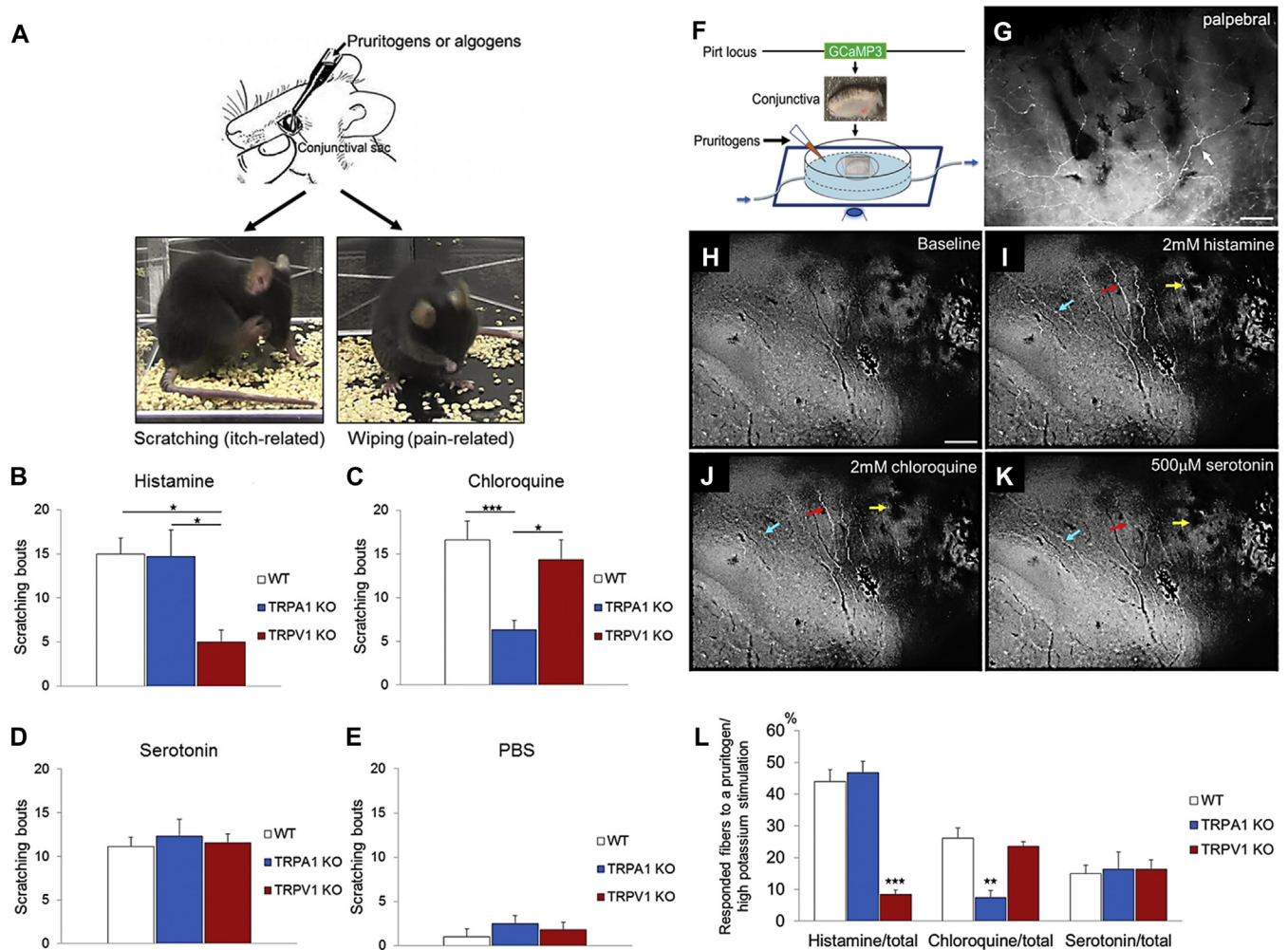
FIG 1. Behavioral and cellular mechanisms of pruritogen-induced ocular itch. **A,** Behavioral distinction between ocular itch and pain in mice. **B,** Histamine-evoked scratching responses were reduced in TRPV1 KO mice (n = 5-9 per group). **C,** Chloroquine-induced scratching behavior was attenuated in TRPA1 KO mice (n = 6-13 per group). **D,** Serotonin evoked comparable number of scratching bouts among 3 genotypes (n = 7-14 per group). **E,** PBS elicited minimal and significantly less scratching responses than any group receiving pruritogen challenge (n = 5-9 per group). **F,** Imaging conjunctival nerve fiber activities using Pirt-GCaMP3 mouse. **G,** Whole-mount immunofluorescence of GCaMP3 signal in a Pirt$^{GCaMP3/+}$ conjunctiva. *White arrow*, GCaMP3$^+$ sensory fiber. **H-K,** Responses of sensory fibers to pruritogens. *Arrows* in different colors indicate conjunctival fibers with differential receptivity to pruritogens. **L,** Percentage of GCaMP3$^+$ conjunctival fibers activated by pruritogens among Pirt$^{GCaMP3/+}$, TRPA1 KO; Pirt$^{GCaMP3/+}$, and TRPV1 KO; Pirt$^{GCaMP3/+}$ mice (n ≥ 5 per group). *Scale bar* represents 100 μm. *P < .05, **P < .01, and ***P < .001.

Involvement of TRPA1-mediated itch pathway in allergic ocular itch was next evaluated using an ocular allergy model. Mast cell–mediated allergic conjunctivitis was induced in mice using an ovalbumin (OVA) sensitization regime (see this article's Methods section in the Online Repository at www.jacionline.org). Topical OVA challenge (250 μg) into unilateral conjunctival sac provoked targeted scratching responses in WT mice (21.6 ± 2.1 bouts; Fig 2, *A*). This itch was caused by allergen (OVA)-specific immune reaction because OVA challenge before sensitization or vehicle treatment after sensitization did not elicit significant scratching responses (Fig 2, *A*). More importantly, our allergic conjunctivitis model recapitulates histologic changes associated with severe seasonal allergy or atopic keratoconjunctivitis in humans,[6] as evidenced by our serial OVA challenges leading to inflammatory cells infiltrations and loss of goblet cells in the

conjunctiva (Fig 2, *B*). Interestingly, in this model, ocular itch was significantly attenuated in TRPA1 KO (10.8 ± 1.9 bouts) and TRPV1 KO (13.3 ± 2.9 bouts) mice, suggesting that both TRPA1 and TRPV1 are required for allergic ocular itch. The observed behavioral changes were not due to defects in mast cell activation of TRPA1 KO or TRPV1 KO mice because mast cell degranulation was comparable among WT, TRPA1 KO, and TRPV1 KO mice (see Fig E2 in this article's Online Repository at www.jacionline.org).

To further explore the potential of TRPA1 as a therapeutic target for allergic conjunctivitis, we examined the effect of pharmacologically blocking TRPA1 in ocular allergy. Compared with the vehicle-treated group (23.4 ± 1.7 bouts), pretreatment with TRPA1 antagonist HC-030031 significantly alleviated allergic ocular itch in mice (10.7 ± 1.3 scratching bouts). More
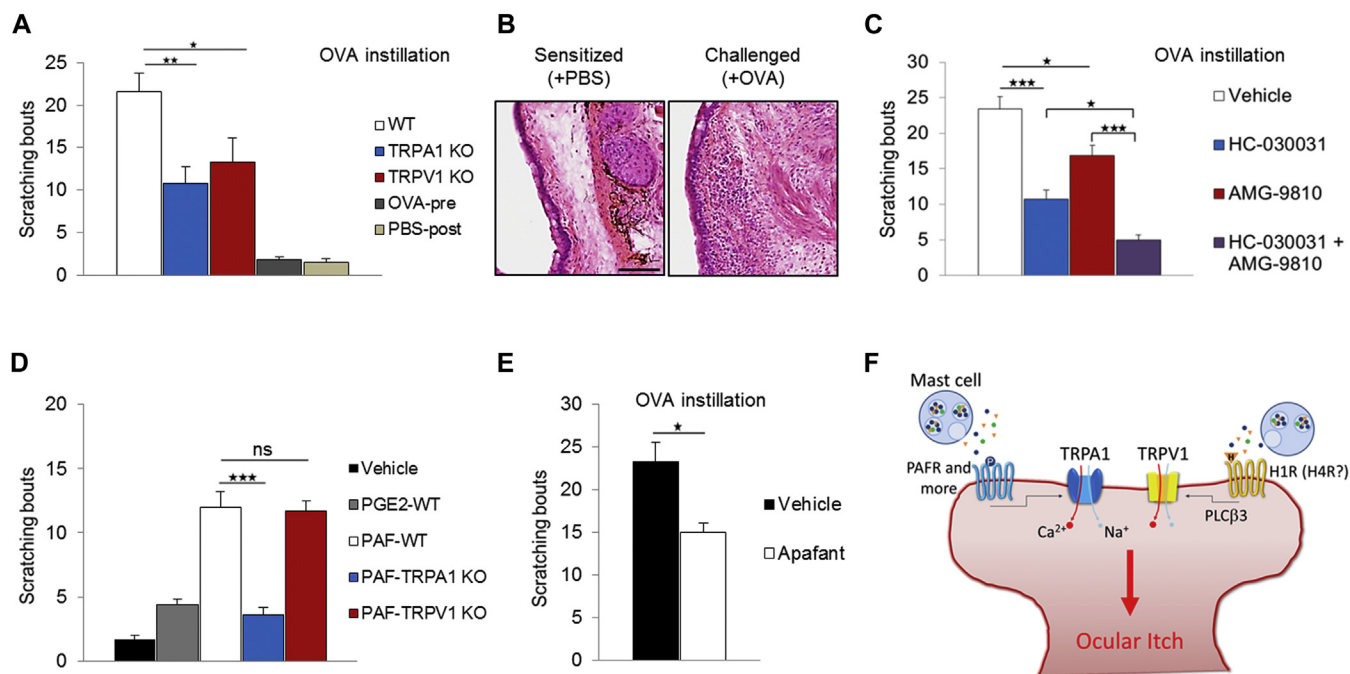
FIG 2. Involvement of TRPA1 and TRPV1 in ocular itch of mast cell–dependent allergic conjunctivitis. **A,** Comparison of scratching behavior among OVA-sensitized WT, TRPA1 KO, and TRPV1 KO mice in response to conjunctival OVA challenge (n = 10-16 per group). **B,** Inflammatory cell infiltration and loss of goblet cell in allergic conjunctiva due to repeated OVA challenges. **C,** Pharmacological antagonism of TRPA1 and TRPV1 channels effectively attenuates ocular itch induced by allergic conjunctivitis (n = 6-9 per group). **D,** Comparison of scratching behavior in response to conjunctival prostaglandin E2 (PGE2) or PAF challenge (n = 6-12 per group). **E,** Topical Apafant alleviates allergic ocular itch (n = 8 per group). **F,** Synergistic activation of TRPA1 and TRPV1 by mast cell mediators confers ocular itch in allergic conjunctivitis. *Scale bar* represents 100 μm. *$P < .05$, **$P < .01$, and ***$P < .001$.

importantly, combined treatment of TRPA1 and TRPV1 antagonists abolished scratching responses to OVA challenge (Fig 2, C), indicating that the TRPA1 pathway complements the TRPV1 pathway in allergic ocular itch, and that combined pharmacological antagonism of TRPA1 and TRPV1 can be an effective and novel therapeutic strategy for allergy-induced ocular itch.

Finally, we investigated potential endogenous histamine-independent itch mediators in ocular allergy. Platelet-activating factor (PAF) and prostaglandin E2 are key inflammatory factors released by mast cells during allergic reaction, and have been shown to cause ocular itch in guinea pigs.[7-9] Following this line of evidence, we found that topical PAF challenge evoked strong scratching responses (12 ± 1.2 bouts), but prostaglandin E2 induced only very mild itch in mice (4.4 ± 0.4 bouts) (Fig 2, D). Interestingly, PAF-induced ocular scratching was reduced in TRPA1 KO but not TRPV1 KO mice, suggesting that TRPA1 is required for PAF-induced itch (Fig 2, D). Indeed, GCaMP3-assisted calcium imaging demonstrated direct activation of a small population of TG neurons by PAF in the presence of TRPA1 (see Fig E3 in this article's Online Repository at www. jacionline.org). To determine whether PAF is involved in allergic ocular itch, mice were pretreated with Apafant, a specific PAF receptor antagonist. Apafant significantly alleviated itch in mice with allergic conjunctivitis (Fig 2, E), substantiating the involvement of PAF in ocular allergic itch. Taken together, our data suggest that PAF is one of the upstream itch mediators for histamine-independent TRPA1 pathway in allergic ocular itch.

The essential role of TRPA1 in allergic ocular itch prompted us to ask whether TRPA1 plays a similar role in allergic skin itch. Allergic skin itch was only marginally reduced in TRPA1 KO mice (154.3 ± 16.1 bouts) compared with WT mice (206 ± 17.5 bouts). Surprisingly, allergic skin itch was not significantly reduced in TRPV1 KO mice (179.4 ± 28.0 bouts), arguing against a critical role of histamine-dependent pathway in this model of skin itch. Our data reveal the first disparity between skin and ocular itch. (For further information, please see Fig E4 in this article's Online Repository at www.jacionline.org.)

Taken together, our results suggest that histamine-independent signaling is equally important as histamine-dependent signaling to mediate ocular itch in allergic conjunctivitis. Current therapeutic strategies for ocular itch management rely heavily on antihistamines and immunosuppressive drugs, and often have limited efficacy. Long-term use of these drugs may be associated with increased risks for ocular complications such as dry eye, glaucoma, and cataract.[1,E1-E5] TRPA1 can potentially serve as a novel therapeutic target for more effective management of allergic ocular itch, especially in cases refractory to conventional treatments. More importantly, our data also imply that targeting both TRPA1 and TRPV1 may achieve an even better and synergistic therapeutic outcome for ocular itch (Fig 2, F), while circumventing untoward effects of current antiocular itch therapies.

Cheng-Chiu Huang, PhD[a]
Yu Shin Kim, PhD[b]
William P. Olson, BS[c]
Fengxian Li, MD[a,d]
Changxiong Guo, BA[a]
Wenqin Luo, MD, PhD[c]
Andrew J. W. Huang, MD, MPH[e]
Qin Liu, PhD[a,e]

From [a]the Department of Anesthesiology and the Center for the Study of Itch, Washington University School of Medicine, St Louis, Mo; [b]the Department of Neuroscience, Johns Hopkins University School of Medicine, Baltimore, Md; [c]the Department of Neuroscience, University of Pennsylvania School of Medicine, Philadelphia, Pa; [d]the Department of Anesthesiology, Zhujiang Hospital, Southern Medical University, Guangzhou, China; and [e]the Department of Ophthalmology and Visual Sciences, Washington University School of Medicine, St Louis, Mo. E-mail: liuqi@anest.wustl.edu.

REFERENCES

1. Ono SJ, Abelson MB. Allergic conjunctivitis: update on pathophysiology and prospects for future treatment. J Allergy Clin Immunol 2005;115:118-22.
2. Metcalfe DD, Baram D, Mekori YA. Mast cells. Physiol Rev 1997;77:1033-79.
3. Raap U, Stander S, Metz M. Pathophysiology of itch and new treatments. Curr Opin Allergy Clin Immunol 2011;11:420-7.
4. Shim WS, Tak MH, Lee MH, Kim M, Kim M, Koo JY, et al. TRPV1 mediates histamine-induced itching via the activation of phospholipase A2 and 12-lipoxygenase. J Neurosci 2007;27:2331-7.
5. Wilson SR, Gerhold KA, Bifolck-Fisher A, Liu Q, Patel KN, Dong X, et al. TRPA1 is required for histamine-independent, Mas-related G protein-coupled receptor-mediated itch. Nat Neurosci 2011;14:595-602.
6. Hu Y, Matsumoto Y, Dogru M, Okada N, Igarashi A, Fukagawa K, et al. The differences of tear function and ocular surface findings in patients with atopic keratoconjunctivitis and vernal keratoconjunctivitis. Allergy 2007;62:917-25.
7. Galli SJ, Tsai M, Piliponsky AM. The development of allergic inflammation. Nature 2008;454:445-54.
8. Gill P, Jindal NL, Jagdis A, Vadas P. Platelets in the immune response: revisiting platelet-activating factor in anaphylaxis. J Allergy Clin Immunol 2015;135:1424-32.
9. Woodward DF, Nieves AL, Spada CS, Williams LS, Tuckett RP. Characterization of a behavioral model for peripherally evoked itch suggests platelet-activating factor as a potent pruritogen. J Pharmacol Exp Ther 1995;272:758-65.

Rigid substrate induces esophageal smooth muscle hypertrophy and eosinophilic esophagitis fibrotic gene expression

To the Editor:

Eosinophilic esophagitis (EoE) is a chronic, food antigen–mediated disease associated with esophageal fibrosis and dysmotility.[1] Esophageal studies using ultrasounds and endoscopic functional luminal probes show increased esophageal rigidity and thickening of the smooth muscle (SM) layers, indicating hypertrophy.[2-4] During EoE progression, the esophagus undergoes substantial tissue remodeling with fibrosis, leading to clinical complications including strictures and food impactions.[1,4] EoE is induced by inflammation, but the consequences of tissue remodeling can remain even after the inflammation is treated, suggesting the role of a fibrotic extracellular matrix (ECM) in the chronic nature of the disease. Fibrosis promotes remodeling of ECM, a substrate for adherent cells composing the tissue, often resulting in increased ECM rigidity. Changes in substrate rigidity have been shown to affect multiple cellular functions important for development, tissue homeostasis, and progression of some diseases including cancer.[5-7] Given the increased esophageal rigidity in EoE, we investigated the effect of cell substrate rigidity on the morphology, size, and gene transcription of cultured normal longitudinal smooth muscle (LSM) cells.

To control the rigidity of the substrate for primary human donor esophagus-derived LSM cells, we used SoftSubstrates silicone gels (MuWells, San Diego, Calif) of defined, physiologically relevant rigidities (Young's Moduli, E, of 0.8, 3, 24, and 48 kPa) (see this article's Methods section in the Online Repository at www.jacionline.org). We found that esophageal LSM cells cultured on a stiffer substrate exhibited decreased cell elongation, more pronounced actin filaments, and larger size compared with cells plated on softer substrates (Fig 1, *A* and *B*). The cell-spreading area was also significantly greater on increasingly rigid matrix ($P = .003$) (Fig 1, *C*). Taken together, our data indicate that SM cells on a rigid matrix have a phenotype consistent with increased contraction and/or hypertrophy.

Phospholamban (PLN), an integral membrane protein regulating the sarcoendoplasmic reticulum calcium channel Serca2, is essential for cardiac contractility and is upregulated in the esophageal muscularis mucosa in pediatric subjects with EoE.[8,9] Our recent work has also identified PLN as an important player in TGFβ1-mediated esophageal SM cell and myofibroblast contraction.[8] To investigate the effects of a rigid matrix on PLN expression, we measured the transcriptional level of PLN in LSM cells plated on substrates of $E = 0.8, 3, 24$, and 48 kPa and found it to be monotonically increased by substrate rigidity (Fig 2, *A*). To understand the role of PLN in regulating SM cell size and morphology, we used a stable transgenic primary human esophageal SM cell line expressing PLN under the control of a doxycycline-inducible promoter (see this article's Methods section in the Online Repository). Using these cells, we found that SM cells overexpressing PLN had decreased elongation and increased cell size on flow cytometry analysis (Fig 2, *B* and *C*). Therefore, upregulation of PLN expression is sufficient to induce morphological changes in SM similar to those observed on rigid substrates.

The pattern of gene expression in LSM cultured on rigid cell substrate was strikingly reminiscent of a subset of TGFβ1-induced genes including PLN, collagen I, and αSMA (Fig 2, *D* and *E*). However, the expression of TGFβ1 itself and other TGFβ1-induced genes such as plasminogen activator inhibitor-1 was not affected by the rigidity of the cell substrate (Fig 2, *D*). Therefore, cellular responses to substrate rigidity are likely to be controlled by signaling pathways with upstream molecular player(s) other than TGFβ1.

In summary, we report here that a rigid cell substrate induces morphological and transcriptional changes in SM cells of the esophagus consistent with EoE. This finding challenges the paradigm of EoE pathogenesis as almost exclusively inflammation-dependent. In addition, the induction of collagen I, a structural component of the esophageal ECM, by a rigid matrix suggests that rigidity can potentially cause a positive feedback loop for fibrosis. We also demonstrate that PLN may be a key molecular player in rigid substrate–induced cellular hypertrophy because its expression increased monotonically with increasingly rigid substrate in parallel with cell size. Moreover, we demonstrated that PLN overexpression is sufficient

METHODS

Animals

TRPV1 KO (*Trpv1^tm1Jul*/J, RRID:MGI_MGI:3834761), TRPA1 KO (*Trpa1^tm1Kykw*, RRID:MGI_MGI:3625358), and Pirt^GCaMP3/+ mice were backcrossed to C57BL/6 mice for at least 6 generations and maintained in the congenic background. TRPV1^PLAP/+ mice (*Trpv1^tm2Bbm*/J, RRID:IMSR_JAX:017623) were purchased from the Jackson Laboratory (Bar Harbor, Me). TRPM8^EGFPf/+ mice were gifts from Dr Gina Story. Eight- to 12-week-old males were used for behavioral tests. All experimental procedures were performed in accordance with protocols approved by the Animal Studies Committee at the Washington University School of Medicine.

Behavioral assays

Experimenters were masked to all mouse genotypes. For ocular itch model, 2.5 μL of testing compounds or vehicle was applied to an inferior conjunctival sac using a micropipette tip after acclimation. For skin itch model, 50 μL of histamine (322 μg), chloroquine (206 μg), or serotonin (10.6 μg) in PBS was injected intradermally around the nape of the back. Individual mouse was placed in a rodent behavior chamber. Scratching and wiping behaviors were video-recorded for 30 minutes and documented. A *single scratching bout* was defined as the animal lifting its hindpaw, scratching the treated area (typically multiple times within seconds), and putting the hindpaw to the floor or to its mouth. A *wiping bout* was defined as the animal lifting its forelimb, wiping the ocular area, and returning to its original start position. Histamine dihydrochloride, chloroquine diphosphate salt, serotonin hydrochloride, and allyl isothiocyanate were purchased from Sigma (St Louis, Mo). PAF and prostaglandin E2 were purchased from Cayman Chemical (Ann Arbor, Mich), dissolved in ethanol, and used at 100 μM. TRPV1 antagonist AMG-9810, TRPA1 antagonist HC-030031, and platelet-activating factor receptor antagonist Apafant were purchased from Tocris Bioscience (Bristol, United Kingdom). For behavioral pharmacology studies, 3 μL of 100 μM AMG-9810 (stock solution 50 mM in ethanol) dissolved in saline with 0.1% Tween-80, 200 μM HC-030031 (stock solution 100 mM in dimethyl sulfoxide) in saline, or both antagonists combined was topically applied to the lower conjunctival sac 10 minutes before OVA challenge. Apafant was used at 500 μM (stock solution 100 mM in ethanol). Control groups were treated with the corresponding vehicle.

Calcium imaging

For whole-mount imaging of the conjunctiva, palpebral to fornical conjunctiva devoid of the hairy eyelid skin were isolated in cold, oxygenated (5% CO_2, 95% O_2) dissection buffer (composition in mM: sucrose 209, KCl 2, NaH_2PO_4 1.25, $MgCl_2$ 5, $NaHCO_3$ 26, glucose 10, and $CaCl_2$ 0.5) and recovered in recording buffer (composition in mM: NaCl 126, KCl 2.5, NaH_2PO_4 1.4, $MgCl_2$ 1.2, $NaHCO_3$ 25, dextrose 11, and $CaCl_2$ 2.4) at room temperature (~25°C) for at least 30 minutes before test. Testing compounds were either perfused into the imaging chamber through a gravity-based delivery system (histamine, chloroquine, and KCl) or bath applied (serotonin and capsaicin). Calcium responses were acquired by an inverted Nikon fluorescence microscope with a CoolSnap HQ2 CCD camera (Photometrics, Tucson, Ariz). Data were quantified offline with the Nikon-NIS program. A minimal 10% increase in $\Delta F/F_0$ in GCaMP3 activity was used to threshold nerve terminal activity. *Single nerve fiber activity* was defined as an increase in the fluorescence intensity of a single identifiable fiber within 30 seconds of delivering chemicals. Any fluorescence changes before chemical application or after bath wash during image acquisition were omitted. Live sensory fibers or TG neurons were identified by eliciting depolarization with 100 mM KCl at the end of each experiment.

Mouse model of mast cell–dependent allergy

OVA from chicken egg white from Sigma was diluted in sterile PBS to 0.02% (w/v) and emulsified with an equal volume of Imject Alum (Thermo Scientific, Rockford, Ill) immediately before use. Mice were injected with 200 μL of OVA/alum mixture intraperitoneally on the 1st and 10th days for sensitization. Sensitized mice were topically challenged with 250 μg OVA/PBS in the lower conjunctival sac, or intradermally injected with 50 μg OVA/PBS in the back skin, on the 17th day after acclimation. Scratching and wiping behaviors were video-recorded for 30 minutes immediately after OVA challenge and analyzed manually.

DiI injection and histology

In anesthetized mice, DiI solution (150 ng/μL dissolved in dimethyl sulfoxide and 1:5 diluted in sterile saline) was injected via a pulled glass pipette into the subconjunctival space (palpebral conjunctiva) of both lower eyelids. Five days after DiI injection, mice were transcardially perfused with PBS followed by 4% paraformaldehyde in PBS. Whole-mount conjunctiva staining for placental alkaline phosphatase was adapted from published protocols.[E6] Immunofluorescence against green fluorescent protein (GFP) or TRPV1 was performed on sucrose-protected cryosections (15 μm). In brief, after blocking, sections were incubated at 4°C overnight in rabbit anti-GFP antibody (Life Technologies, Eugene, Ore; catalogue no. A11122, RRID:AB_10073917) or rabbit anti-TRPV1 antibody (Neuromics, Edina, Minn; catalogue no. RA14113-100, RRID:AB_2255202) at 1:1000 dilution in PBS containing 0.1% Triton-X100 (PBST). Sections were then washed and incubated at room temperature for 2 hours in Alexa 488–conjugated secondary antibodies (Life Technologies; catalogue no. A11008, RRID:AB_10563748). Of note, GCaMP3 is a fusion protein of GFP and calmodulin, and therefore can be recognized by the anti-GFP antibody. After final washes, slides were mounted with Fluoromount-G (Southern Biotech, Birmingham, Ala). In the mast cell–dependent allergy model, conjunctival and skin mast cells were identified by staining endogenous heparin with Alexa 488–conjugated avidin (Life Technologies; catalogue no. A21370).

In situ hybridization

TG were dissected and rapidly frozen in optimal cutting temperature medium on a dry-ice/ethanol bath. Twenty-micrometer cryosections were collected and allowed to dry for at least 2 hours at room temperature. DiI fluorescence was imaged before *in situ* hybridization. Following imaging, all steps before hybridization were carried out under Rnase-free conditions. Sections were immersion-fixed in freshly made 4% PFA for 20 minutes at room temperature. Slides were then washed in fresh-Diethylpyrocarbonate (DEPC) PBS (1:1000 DEPC in PBS immediately before use), followed by wash in DEPC-pretreated PBS (1:1000 DEPC in PBS overnight, followed by autoclaving). Sections were immersed in freshly boiled antigen retrieval solution (10 mM citric acid, 0.05% Tween-20, pH = 6.0 with 1:1000 diluted DEPC) in a 95°C water bath for 20 minutes, and then allowed to cool at room temperature for 30 minutes. Sections were washed in DEPC-pretreated PBS, incubated in Proteinase K (25 μg/mL in DEPC-pretreated H_2O) for 5 minutes, followed by washes in fresh-DEPC PBS and DEPC-pretreated PBS. Sections were then incubated in freshly made acetylation solution (0.1 M triethanolamine, 0.25% acetic anhydride in DEPC-pretreated H_2O) for 10 minutes at room temperature. Next, slides were prehybridized in hybridization buffer (50% formamide, 5 × SSC, 0.3 mg/mL yeast tRNA, 100 μg/mL heparin, 1 × Denhardt's, 0.1% Tween-20, 0.1% 3-[(3-cholamido-propyl)dimethylammonio]-1-propanesulfonate (CHAPS), 5 mM EDTA in Rnase-free H_2O) at 62°C in a humidified chamber for 30 minutes. Following prehybridization, 1 to 2 ng/μL of Digoxigenin (DIG)-labeled riboprobe diluted in hybridization buffer was placed on the slide. Slides were incubated overnight under Parafilm coverslips at 62°C and then washed in 0.2 × SSC at 68°C. Following hybridization, slides were blocked in 20% lamb serum in PBST at room temperature for 1 hour. Sections were then incubated with AP-conjugated anti-DIG antibody (1:1000; Roche, catalogue no. 11093274910) in blocking buffer overnight at 4°C. Slides were washed in PBST and incubated overnight in darkness in alkaline phosphatase buffer: 100 mM Tris, pH 9.5, 50 mM $MgCl_2$, 100 mM NaCl, 0.1% Tween-20, 5 mM levamisole, 0.34 mg/mL 4-Nitro blue tetrazolium (Roche, Nutley, NJ; catalogue no. 11383213001) and 0.17 mg/mL 5-bromo-4-chloro-3-indolyl-phosphate (Roche, catalogue no. 1138221001). Slides were then repeatedly rinsed in ddH_2O, dried at 37°C for 1 hour, dehydrated in xylenes, and covered in Permount (Fisher Scientific, Pittsburgh, Pa; catalogue no. SP15).

Data analysis

Data are shown as means ± SEM. One-way ANOVA was used for initial analyses among groups, followed by Turkey *post hoc* tests. Differences between groups were considered statistically significant when $P < .05$.

REFERENCES

E1. Ciprandi G, Buscaglia S, Cerqueti PM, Canonica GW. Drug treatment of allergic conjunctivitis: a review of the evidence. Drugs 1992;43:154-76.

E2. Friedlaender MH. Ocular allergy. Curr Opin Allergy Clin Immunol 2011;11: 477-82.

E3. Scheurer ME, El-Zein R, Thompson PA, Aldape KD, Levin VA, Gilbert MR, et al. Long-term anti-inflammatory and antihistamine medication use and adult glioma risk. Cancer Epidemiol Biomarkers Prev 2008;17:1277-81.

E4. Scheurer ME, Amirian ES, Davlin SL, Rice T, Wrensch M, Bondy ML. Effects of antihistamine and anti-inflammatory medication use on risk of specific glioma histologies. Int J Cancer 2011;129:2290-6.

E5. Amirian ES, Marquez-Do D, Bondy ML, Scheurer ME. Antihistamine use and immunoglobulin E levels in glioma risk and prognosis. Cancer Epidemiol 2013;37:908-12.

E6. Cavanaugh DJ, Chesler AT, Jackson AC, Sigal YM, Yamanaka H, Grant R, et al. Trpv1 reporter mice reveal highly restricted brain distribution and functional expression in arteriolar smooth muscle cells. J Neurosci 2011;31:5067-77.
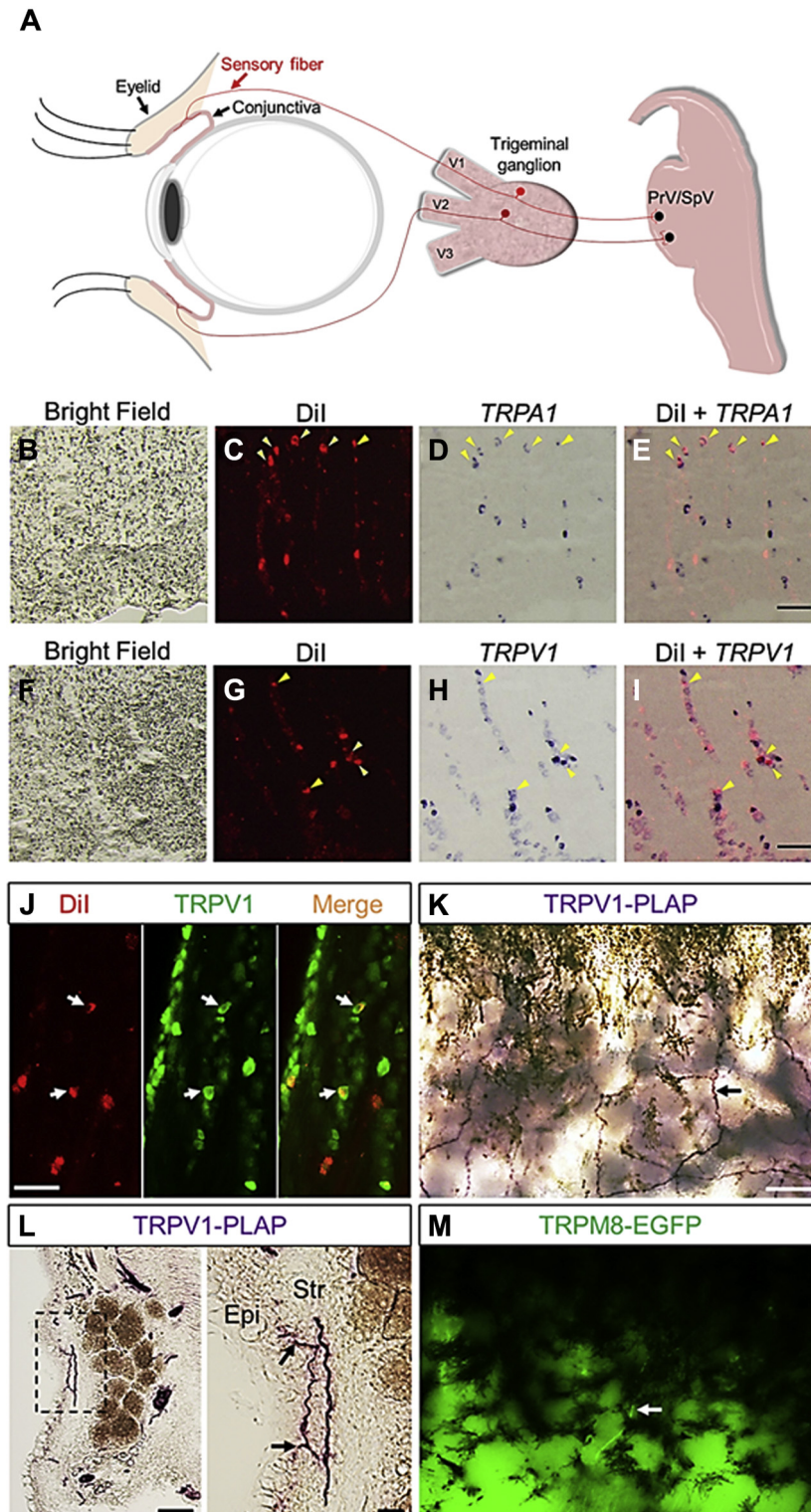
FIG E1. Sensory innervations of the mouse conjunctiva. **A,** Diagram of ocular itch pathway from conjunctival sensory fibers to brainstem nuclei (PrV/SpV). **B-I,** Detection of *TRPA1* and *TRPV1* mRNA expression by *in situ* hybridization. TG neurons innervating the conjunctiva are labeled by the retrograde tracer DiI. *Yellow arrowheads* indicate TRPA1^{+}/DiI[+] or TRPV1^{+}/DiI^{+} neurons in the TG. **J,** Detection of TRPV1 protein in TG neurons innervating the conjunctiva by immunofluorescence. *White arrows,* TRPV1^{+}/DiI^{+} TG neurons. **K,** Whole-mount histochemical staining of TRPV1-PLAP in mouse conjunctiva. *Black arrow,* TRPV1^{+} sensory fiber. **L,** Relation of TRPV1^{+} nerve terminals to conjunctival epithelium. *Black arrows,* TRPV1^{+} terminals. **M,** Whole-mount immunofluorescence of GFP signal in a TRPM8[EGPf/+] conjunctiva. *White arrow,* TRPM8^{+} sensory fiber. *Epi,* Epithelium; *Str,* stroma. *Scale bars* represent in *B* to *I,* 100 μm; *J,* 50 μm; *K* and *M,* 100 μm; *L,* 20 μm.
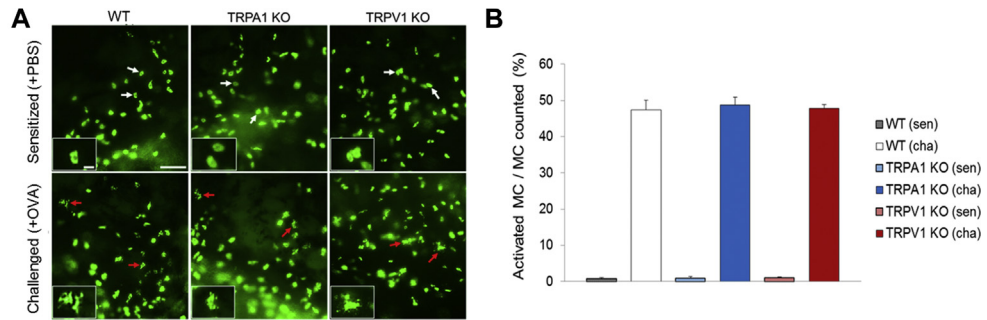
FIG E2. TRPA1 and TRPV1 are not required for allergen-induced mast cell degranulation. **A,** No difference in conjunctival mast cell degranulation was observed among 3 genotypes. *White arrows*, OVA-sensitized conjunctival mast cells. *Red arrows*, activated conjunctival mast cells by OVA. *Scale bars* represent 100 μm; 20 μm in insets. **B,** Quantitative analysis of mast cell degranulation among 3 genotypes. N ≥ 3 mice and >200 mast cells were analyzed per group.
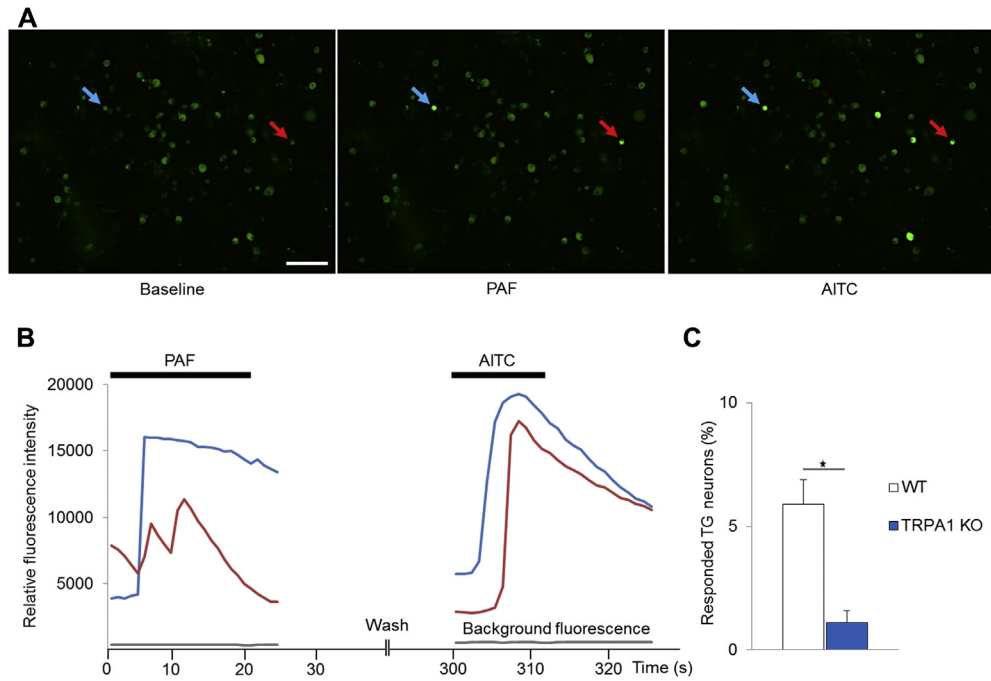
FIG E3. TRPA1 is required for PAF-induced Ca^{2+} mobilization in sensory neurons. **A,** PAF activates a subset of TRPA1^{+} neurons from the TG. Increased Ca^{2+} mobility on PAF (10 μM) and allyl isothiocyanate (AITC, TRPA1 agonist, 100 μM) treatment in Pirt$^{GCaMP3/+}$ TG neurons. *Arrows* indicate neurons that are sensitive to both PAF and AITC. **B,** Calcium traces of TG neurons that responded to PAF and AITC in *A*. **C,** PAF-induced Ca^{2+} mobility in TG neurons was significantly attenuated in TRPA1 KO mice. N $\geq$ 3 mice and >400 TG neurons were analyzed per group. *Scale bar* represents 100 μm. *P < .05.
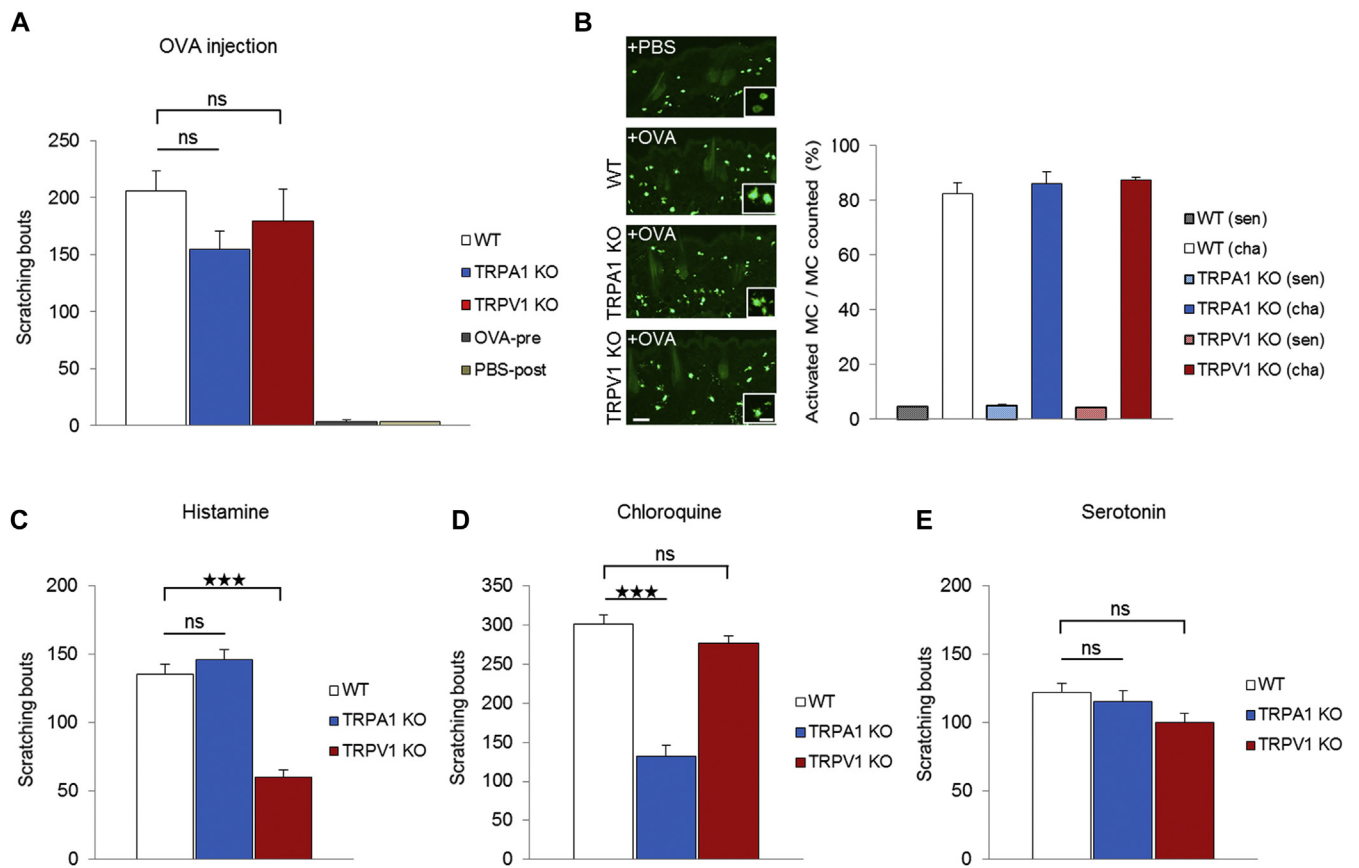
FIG E4. Behavioral responses of pruritogen-induced and allergy-induced skin itch. **A,** Scratching responses induced on the intradermal injection of OVA solution into the *back skin* in an allergic skin itch model. TRPA1 KO mice showed only marginally fewer scratching bouts than did the WT group, but did not differ from the TRPV1 KO mice (n = 9-14 per group). **B,** No difference in degranulation of skin mast cell was observed among 3 genotypes. N ≥ 3 mice and >500 mast cells were analyzed per group. **C-E,** Histamine-dependent itch was reduced in TRPV1 KO mice. Chloroquine-dependent itch was reduced in TRPA1 KO mice. No difference was shown among genotypes in serotonin-induced itch (n = 7-12 per group). *Scale bars* represent 50 μm; 10 μm in insets. *ns,* Not significant. ***$P < .001$.